Hindawi
Advances in Civil Engineering
Volume 2018, Article ID 1260787, 9 pages
https://doi.org/10.1155/2018/1260787

Research Article

Numerical Calculation Analysis of the Structural Stability of Cemented Fill under Different Cement-Sand Ratios and Concentration Conditions

Kang Zhao,[1,2,3] **Qiang Li**,[1] **Yajing Yan**,[1] **Keping Zhou**,[2] **Shuijie Gu**,[1] **and Shengtang Zhu**[1]

[1]*School of Architectural and Surveying & Mapping Engineering, Jiangxi University of Science and Technology, Ganzhou 341000, China*
[2]*School of Resources and Safety Engineering, Central South University, Changsha, Hunan 410083, China*
[3]*Jiangxi Provincial Key Laboratory of Geotechnical Engineering and Environmental Disaster Control, Ganzhou 341000, China*

Correspondence should be addressed to Kang Zhao; zhaok_666666@163.com

Received 6 May 2018; Revised 3 July 2018; Accepted 24 July 2018; Published 27 August 2018

Academic Editor: Gaofeng Zhao

The effect of lime-sand ratio and slurry concentration on the mechanical properties of backfills is important. To achieve green and high-efficiency mining, accurately determining the optimum ratio of cemented tailings for certain tungsten tailings and ensuring the safety and stability of the mine stope structure are important. The cement-sand ratios used in this research were 1 : 6 and 1 : 8. The mechanical properties were evaluated by using 68%, 72%, and 78% of tailing cemented filling materials. The corresponding physical and mechanical parameters were obtained through uniaxial compression, splitting, and shearing mechanical experiments on the backfill specimens. FLAC^{3D} was used to investigate the mechanical properties of cement-filled pillars and the stability of supporting surrounding rocks on the basis of the mine's current room pillar structure size parameters and mining sequence. The key factors that affect the stability of the goaf were analyzed by evaluating the plastic zone area of the stope, maximum and minimum principal stresses, and displacement change. The structural characteristics of stope structures and changes of rock mass damage were obtained under different cement-tailing ratios and concentrations. A cemented backfill with a cement-tailing ratio of 1 : 8 and a concentration of 68% was selected as the best solution for the mine in terms of safety and economic considerations.

1. Introduction

Since the 1950s, the environmental protection requirements of various countries have increased considerably, and the loss and depletion of scarce and expensive minerals should be reduced due to the increasing depth of underground mining. The development of green, safe, and efficient mining technology has attracted considerable attention from scholars and engineering technicians from various countries. In the 1950s and 1960s, cemented filling of new processes went into production, thereby overcoming the shortcomings of previous mining methods and increasing the applications of the filling mining method annually [1, 2]. The filling method has remarkable advantages over other methods in controlling surface deformation and improving ore recovery [3]. The influence of the filling mining method on the stability of the mine and the induced surface settlement deformation are closely related to the strength of the cemented backfill. Therefore, the determination of cemented backfill strength is a crucial part of the filling mining method. Empirical, theoretical, finite element, and rock mechanics numerical analyses are generally used for the design of cemented backfill strength [4]. Fall [5, 6] studied the mechanical properties and failure characteristics of backfills. Li [7] studied the factors that influence the strength of tailing backfills by using the orthogonal tests and analyzed the strength characteristics of tailing cemented backfills. Liu [8] analyzed the deformation characteristics and failure of tailing cemented backfills with different proportions and established damage constitutive equations for the backfills

with damage mechanics. Li et al. [9] used test methods to investigate the mechanical properties and influencing factors of cemented backfills when vermiculite was used as the filling material and cement-water glass was used as the grouting cement to perform cementation in the goaf. Xu et al. [10] assessed the deformation law during the compaction process of vermiculite-fly ash filling materials and obtained the optimal ratio of vermiculite and fly ash fillers. Shi et al. [11] evaluated the sensitivity of cement, fly ash, and coal gangue with different ratios and paste concentrations on various performance indexes of coal gangue and gypsum body filling and the trend of each index with each factor. These research achievements have ensured mining safety to a certain extent and promoted the development of filling and mining technologies. However, most of these studies use empirical methods or empirical analogy methods to determine the composition and strength design of backfilling materials, thereby frequently resulting in cement waste or the failure of backfills to meet the actual requirements for ground pressure control. This study conducts indoor experiments and numerical analysis to investigate the stability of a tailing cement filling stope structure. The different ratios are compared and evaluated by analyzing the change of the stope plastic zone, displacement, and the distribution of maximum and minimum principal stresses. The filling effect of the filling body concentration is determined to select the best ratio.

2. Engineering Geology Overview

A large-scale tungsten mine in Jiangxi Province located in the Jiulian Mountains bordering Guangdong and Jiangxi is used as the study area. The mining area is in the valley topography, and its highest elevation peak is 1,043 m. The mining area has mainly slope quaternary modern products, and its eluvium and alluvium are located in the northwest end flap of Gukeng large anticline that plunges to the southwest direction. The rock strata direction in the area varies with the site structure. Most of the folds are in the northeast-southwest and near north-south directions, and the inclination and trend are remarkably changed. A large number of faults, joints, and fractures are found in the rock formation, which becomes a space for deformation and compression. The middle part of the mining area is mainly distributed in the structural development zone and weathered layer. Many cracks and fragments are found in the rock mass structure due to the influence of structural development and high degree of weathering. The rock mass structure is partially muddy and its bearing capacity is low.

3. Experiment on Backfill Mechanical Properties

3.1. Making Backfills. The mine has a long history of mining, and many tailings have been produced during the mining process. Therefore, the use of tailings as a filling material for locally sourced materials reduces costs, protects the environment, and facilitates construction. The test piece used in this study is obtained from the graded tailings of a mine in Jiangxi Province, and ordinary Portland cement PO 32.5 (32.5) is used as the cementing material. The respective lime-sand ratios and slurry mass concentrations are 1 : 6 and 68%, 1 : 6 and 72%, 1 : 6 and 76%, 1 : 8 and 68%, 1 : 8 and 72%, and 1 : 8 and 78%. Then, a cylindrical body with a diameter of 50 mm and a height of 100 mm is cast in a compressive test piece in accordance with the relevant regulations. The tensile test piece is a cylinder with a diameter of 50 mm and a height of 50 mm. The designed curing age is 28 days. Part of the molded specimen is shown in Figure 1.

Figure 1: Part of the molded specimen.

3.2. Cemented Backfill Mechanics Experiment. Uniaxial compression, splitting failure, and shear tests of the cemented backfill are conducted by using a digitally controlled electrohydraulic servosystem RMT-150C rock mechanics tester. For the processing and analysis of test data, the mechanical parameters of the backfill under different lime-sand ratios and concentrations are shown in Table 1.

The uniaxial compressive strength, elastic modulus, Poisson's ratio, and other basic physical and mechanical parameters of the main backfill are experimentally obtained. The compressive strength and elastic modulus of the backfill increase, and Poisson's ratio decreases with the increase in lime-sand ratio and concentration. Basic data, such as cohesion and internal friction angle, are obtained through the shear strength test. On the basis of the mechanical strength parameters of cohesion and internal friction angle obtained in the shear strength test, the cohesion and internal friction angle of the cemented backfill increase with the increase in the concentration and proportion of the cemented backfill. Specifically, the internal friction angle and cohesion of the cemented backfill are directly related to slurry concentration and cement-sand ratios.

4. Stability of Filling Materials with Different Proportions and Concentrations

4.1. Finite Element Simulation Scheme and Model. The reliability of numerical calculation largely depends on the establishment of a computational model; that is, the reliability and rationality depend on the selection of rock mechanical parameters and boundary conditions [12–14].

Table 1: Cemented backfill mechanics experiment results.

Lithology	Compressive strength (MPa)	Tensile strength, σ_t (MPa)	Bulk modulus, K (GPa)	Elastic modulus, E (GPa)	Poisson's ratio, υ	Shear modulus, G (GPa)	Internal friction angle, φ (°)	Cohesion, C (MPa)
Lime-to-sand ratio 1 : 6, concentration 68% backfill (program one)	1.167	1.36	0.26	0.25	0.33	0.09	13.8	0.36
Lime-to-sand ratio 1 : 6, concentration 72% backfill (program two)	1.576	0.17	0.29	0.37	0.29	0.14	18.0	0.51
Lime-to-sand ratio 1 : 6, concentration 78% backfill (program three)	2.098	0.19	0.36	0.57	0.24	0.23	20.2	0.61
Lime-to-sand ratio 1 : 8, concentration 68% backfill (program four)	0.797	0.05	0.11	0.1	0.34	0.04	10.2	0.21
Lime-to-sand ratio 1 : 8, concentration 72% backfill (program five)	0.941	0.07	0.14	0.16	0.31	0.06	15.2	0.38
Lime-to-sand ratio 1 : 8, concentration 78% backfill (program six)	1.113	0.93	0.12	0.19	0.25	0.08	18.2	0.521

4.1.1. Establishment of Numerical Models. On the basis of the problems to be solved in the research and the occurrence of ore bodies combined with the mining methods used in the mine, the optimization model of the structure parameters of the stope considers the mining of a pillar in two mines. The range of disturbance is three to five times the mining scope. The established model dimensions are 900 m in the x axis, 300 m in the y axis, and 500 m in the z axis. The mining block sizes are 25 m in the x axis, 30 m and 200 m in the y axis, and 40 m in the z axis. The model is shown in Figure 2 after a certain rotation. The optimal sizes of stope structure parameters are 18 m for mining houses and 7 m for pillars. On the basis of the actual situation of the mine, the mining sequence model is divided into four pillars of five mines, and the mining sequence is divided by one. The shape of the ore body is simplified based on the ore body shape map provided by the mine, and the requirements for satisfying the calculation and mesh division are considered. The simplified ore body model is shown in Figure 2.

4.1.2. Boundary Conditions. The boundary conditions of the analyzed model are set as the horizontal boundary and vertical speed constraints at the bottom of the model and the horizontal speed constraints of the boundary between the two sides of the model, which are expressed as follows: (1) the model at the bottom $z = 0$ m, the water level is fixed in the x, y, and z directions, and no speed or displacement occurs; (2) the two sides of the model, namely, $x = 0$ m and $x = 900\,\text{m}^2$, are fixed, and no velocity and displacement occur; (3) in the model, $y = 0$ m and $y = 300\,\text{m}^2$ end faces are fixed surfaces, and no velocity or displacement occurs; and (4) the model is a free surface at the surface. To ensure the reliability of the simulation, the initial stress field of the model is generated in accordance with the actual engineering environment. A uniform surface load of 11.73 MPa

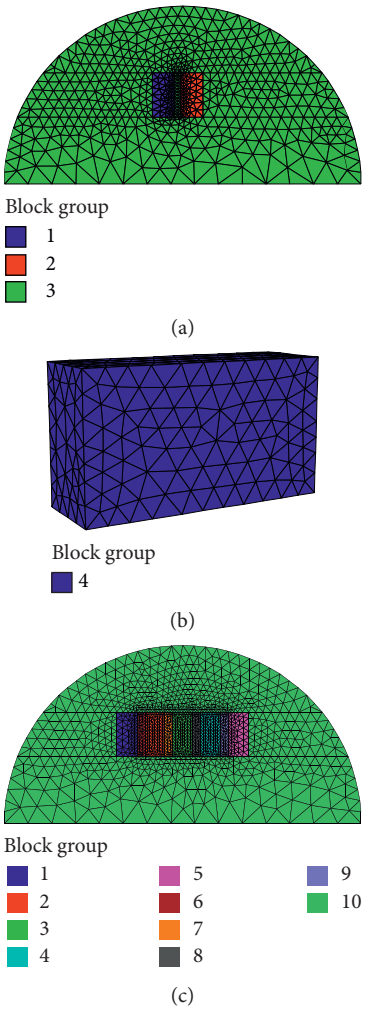

Figure 2: Numerical model: (a) simplified ore body shape; (b) grid model; (c) mining block diagram.

Table 2: Mechanical parameters of the model.

Lithology	Tensile strength, σ_t (MPa)	Volume-weight	Elastic modulus, E (GPa)	Poisson's ratio, υ	Internal friction angle, φ (°)	Cohesion, C (MPa)
Surrounding rocks	2.4	2.75	17.6	0.22	19.58	4.6
Ore rock	1.36	2.77	6.36	0.23	7.66	10.29

was applied to the upper part of the model by combining the results of the previous in situ stress measurement test. Compressive stresses of 19.67 MPa were applied on the two faces perpendicular to the x (length) axis. Compressive stress of 7.73 MPa was applied on the two faces perpendicular to the y (width) axis.

4.1.3. Physical and Mechanical Parameters of Rocks. On the basis of the physicomechanical properties of the ore rock and experimental results, the test results were reduced and the mechanical parameters of the main rock mass were determined by considering the effects of specimen size and the surrounding environment of surrounding rocks, as shown in Table 2.

FLAC^{3D} is used for numerical simulation to analyze the state characteristics and stress and strain of backfills and surrounding rocks and to optimize the backfills. The mechanical parameters of the filling body are obtained from the indoor mechanical test results in Table 1.

4.1.4. Monitoring Point Layout. For convenience of research and analysis, monitoring points are placed at key positions in the calculation model. The variation of the nuggets and surrounding rocks is monitored as a function of ore mining, and the 3D mechanical status and evolution of the nuggets and surrounding rocks are recorded during the mining process. The calculation model places a monitoring point on the roof, as shown in Figure 3. The #1 monitoring point is located in the roof rock and monitors the roof displacement. The #2 monitoring point is located at the junction of the pillar and surrounding rock to monitor the change of body strain in the plastic zone of the pillar.

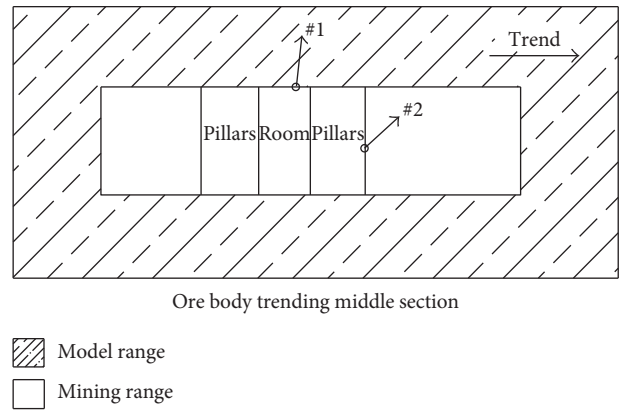

Figure 3: Model monitoring point layout diagram.

4.2. Analysis of FLAC3D Simulation Results

4.2.1. Plastic Zone Analysis. Figure 4 shows the distribution of the plastic zone when the mining sequence was adopted. For the distribution maps of plastic zones of six schemes, the plastic zone mainly concentrates on the side wall boundary of the mine house after the filling of mine house 1. Shear and tensile failures are observed at the top and bottom of the pillar, with a small difference in the shear and tension zones. A relatively large plastic zone appears around mine house 5 due to the stress release phenomenon in the surrounding rock mass during the mining process, and the damage is mainly caused by tensile failure. For the same cement-sand ratio, the tensile failure range of the stope structure gradually decreases and no obvious penetration of the pillar is observed with the increase in the backfill concentration. For the same concentration, the sand-to-sand ratio of 1 : 6 is smaller than that of 1 : 8. Zheng et al. [15] believed that the plastic zone has a close relationship with Poisson's ratio of rock mass. Therefore, the result of Figure 3 and Table 1 shows that the plastic area of backfilling is small after filling when Poisson's ratio is small.

As shown in the plastic zone map, the #2 monitoring point at the tensile stress results in deformation. As shown in the body-strain curve in Figure 5, the body strain decreases, but the difference is insignificant with the increase in concentration under the same lime-sand ratio.

4.2.2. Vertical Displacement Analysis. In the ore mining process, the initial stress balance system of surrounding rocks is destroyed with the continuous mining of ore bodies. In this case, the surrounding rocks should be rebalanced by rock mass deformation under the effect of its internal unbalanced stress. In this process, the accumulated stress in the surrounding rocks is released continuously and transferred externally. The large release or transfer of stress leads to excessive displacement of the rock wall, thereby causing large areas of the roof to fall and resulting in underground mining safety hazards and mining depletion.

After the excavation of the mining house, the original state of stress balance is destroyed, which causes the internal stress of the rock mass to be redistributed until it reaches a new equilibrium state. In the stress rebalancing process, the displacement, deformation, and destruction of the rock mass around the roadway are observed. To analyze the deformation process of the rock mass that surrounds the mine house, the vertical displacements of the top and bottom columns are analyzed through displacement analysis. A comparison of the displacement cloud diagram of six schemes (Figure 6) shows that the roof settlement of each scheme is slightly similar to the maximum value of floor uplift but is slightly different in the distribution area. The vertical displacement of the backfill with a concentration of 76% is small, the

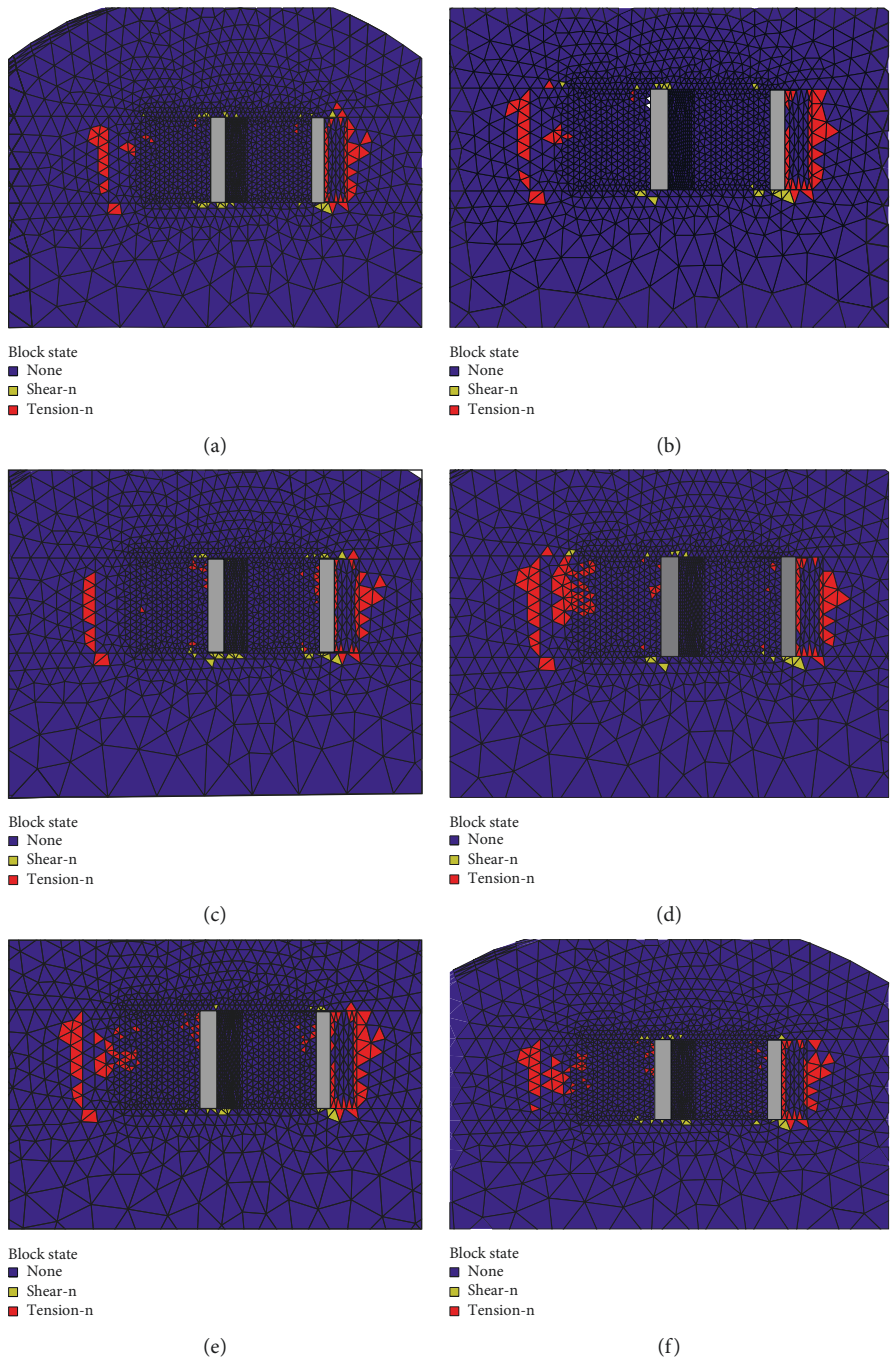

Figure 4: Plastic zone distribution map: (a) cement-sand ratio 1 : 6, backfill concentration 68%; (b) cement-sand ratio 1 : 6, backfill concentration 72%; (c) cement-sand ratio 1 : 6, backfill concentration 78%; (d) cement-sand ratio 1 : 8, backfill concentration 68%; (e) cement-sand ratio 1 : 8, backfill concentration 72%; (f) cement-sand ratio 1 : 8, backfill concentration 72%.

amount of roof subsidence is 2.65 cm, and the amount of bottom uplift is 2.43 cm when the lime-sand ratio is 1 : 6. The vertical displacements of the two other concentrations are relatively large. The vertical displacement is slightly similar when the concentration is constant under different lime-sand ratios.

As shown in the comparison of the effects of mining on the overlying strata in six different width mines in Figure 7, the maximum convergence displacement of the roof gradually increases with the reduction in the proportion and concentration of backfills, but the difference is insignificant. The sinking of the roof is mainly due to the movement of the rock mass around the empty area to the free space under its own weight and internal stress, and this phenomenon gradually extends upward. The subsidence of the roof is controlled, and the extent of overlying strata affected by the overlying strata is relatively reduced due to the enhanced support of pillars and cemented backfills. The subsidence degree of the overlying

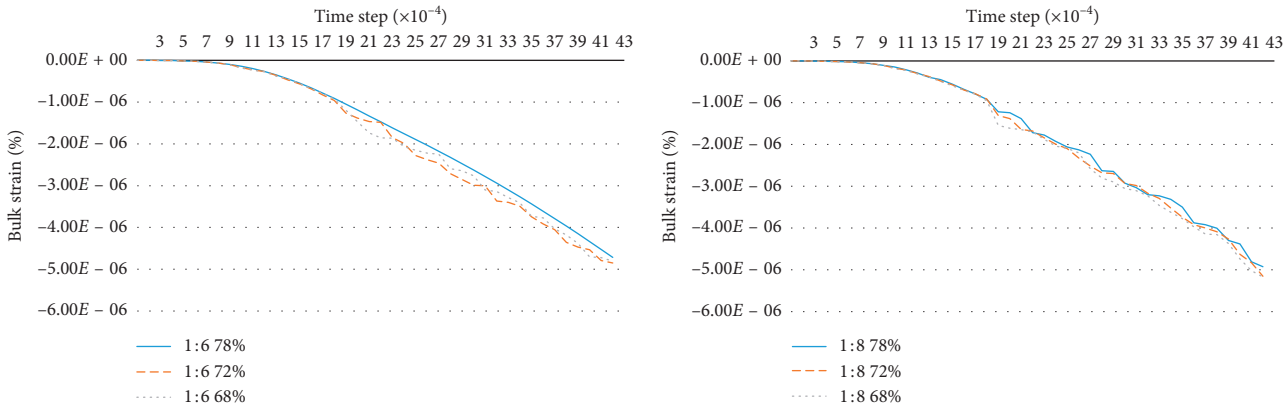

Figure 5: #2 monitoring point bulk strain-time step graph.

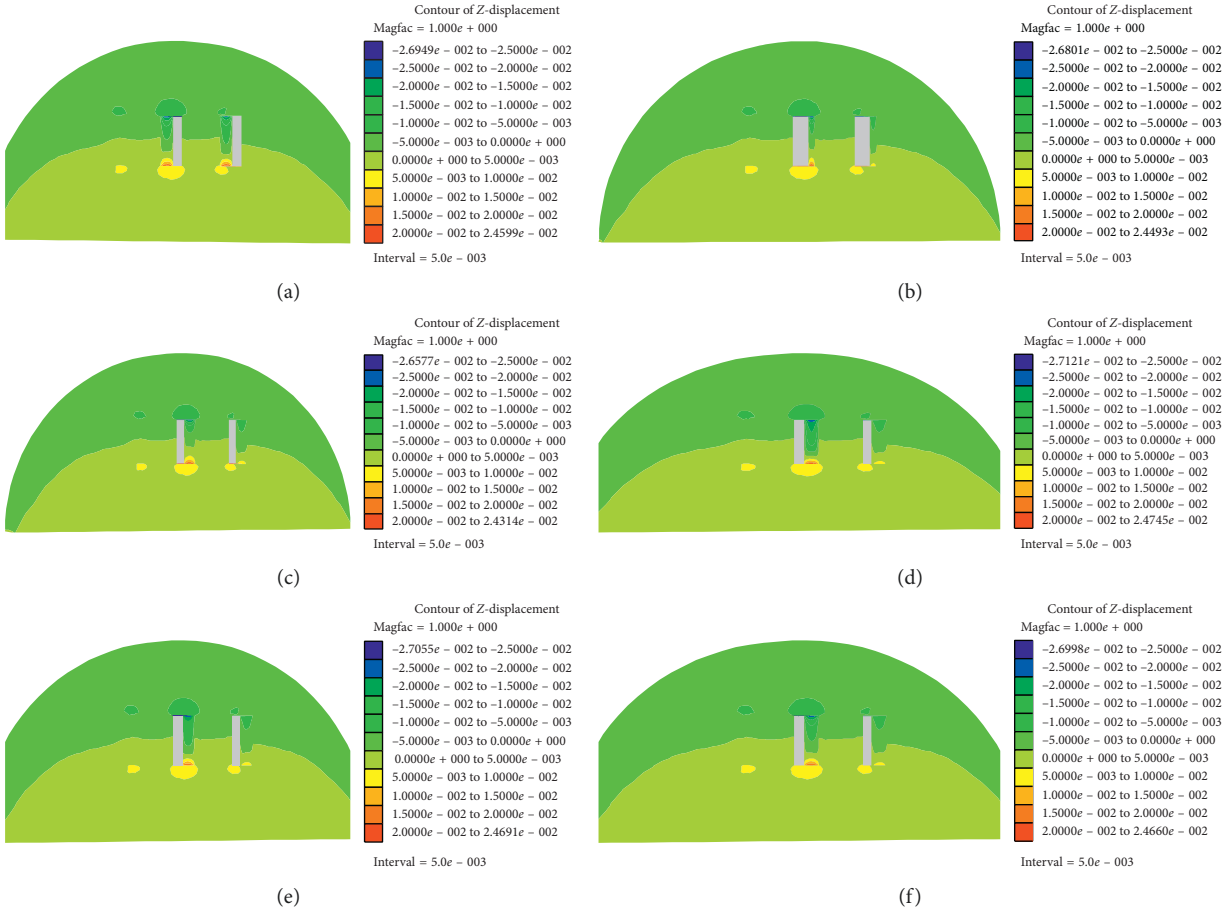

Figure 6: Vertical displacement cloud: (a) cement-sand ratio 1 : 6, backfill concentration 68%; (b) cement-sand ratio 1 : 6, backfill concentration 72%; (c) cement-sand ratio 1 : 6, backfill concentration 78%; (d) cement-sand ratio 1 : 8, backfill concentration 68%; (e) cement-sand ratio 1 : 8, backfill concentration 72%; (f) cement-sand ratio 1 : 8, backfill concentration 78%.

strata is relatively weak. By contrast, the support strength is gradually enhanced due to the mine's main support structure and the support of cemented backfill during the pillar mining phase.

4.2.3. Analysis of Maximum and Minimum Principal Stresses. Figure 8 shows a comparison of the maximum principal stress of the filled pillars of six schemes. As shown in the figure, the bottom of the mining area is under pressure and

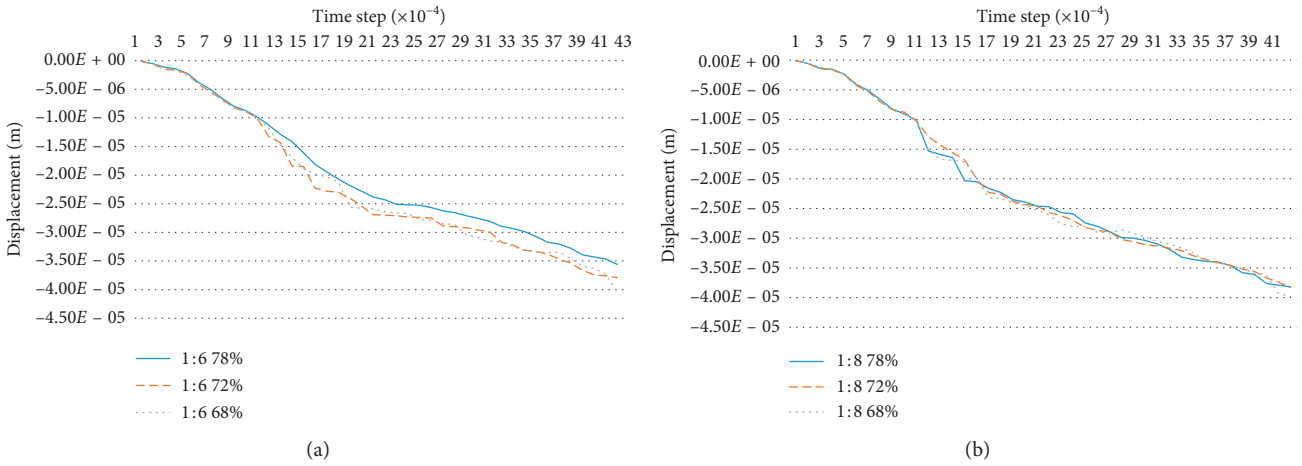

Figure 7: #1 monitoring point vertical displacement-time step curve.

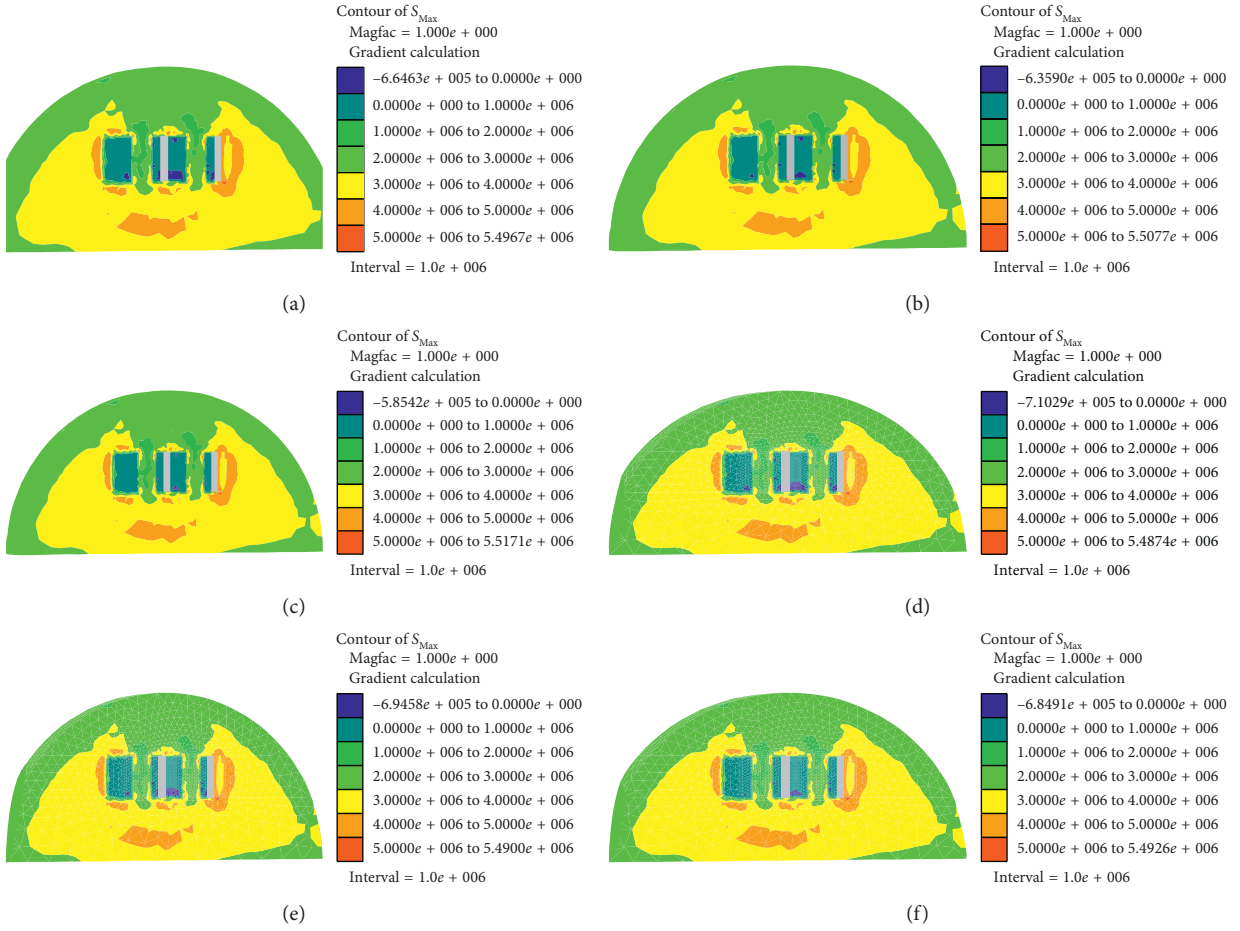

Figure 8: Maximum principal stress cloud: (a) cement-sand ratio 1 : 6, backfill concentration 68%; (b) cement-sand ratio 16, backfill concentration 72%; (c) cement-sand ratio 1 : 6, backfill concentration 78%; (d) cement-sand ratio 1 : 8, backfill concentration 68%; (e) cement-sand ratio 1 : 8, backfill concentration 72%; (f) cement-sand ratio 1 : 8, backfill concentration 78%.

the surrounding rock mass distributes tensile stress, which is mainly related to the distribution of ground stress and stress release of rock mass. The maximum tensile stress of each scheme changes slightly. The tensile stress is in the range of 5.48–5.50 MPa. However, the compressive and tensile range of the model decreases with the increase in filler concentration when the lime-sand ratio of the filler of the same concentration is 1 : 8, and the pressure and tension ranges are smaller than when the ratio of lime-sand ratio is 1 : 6.

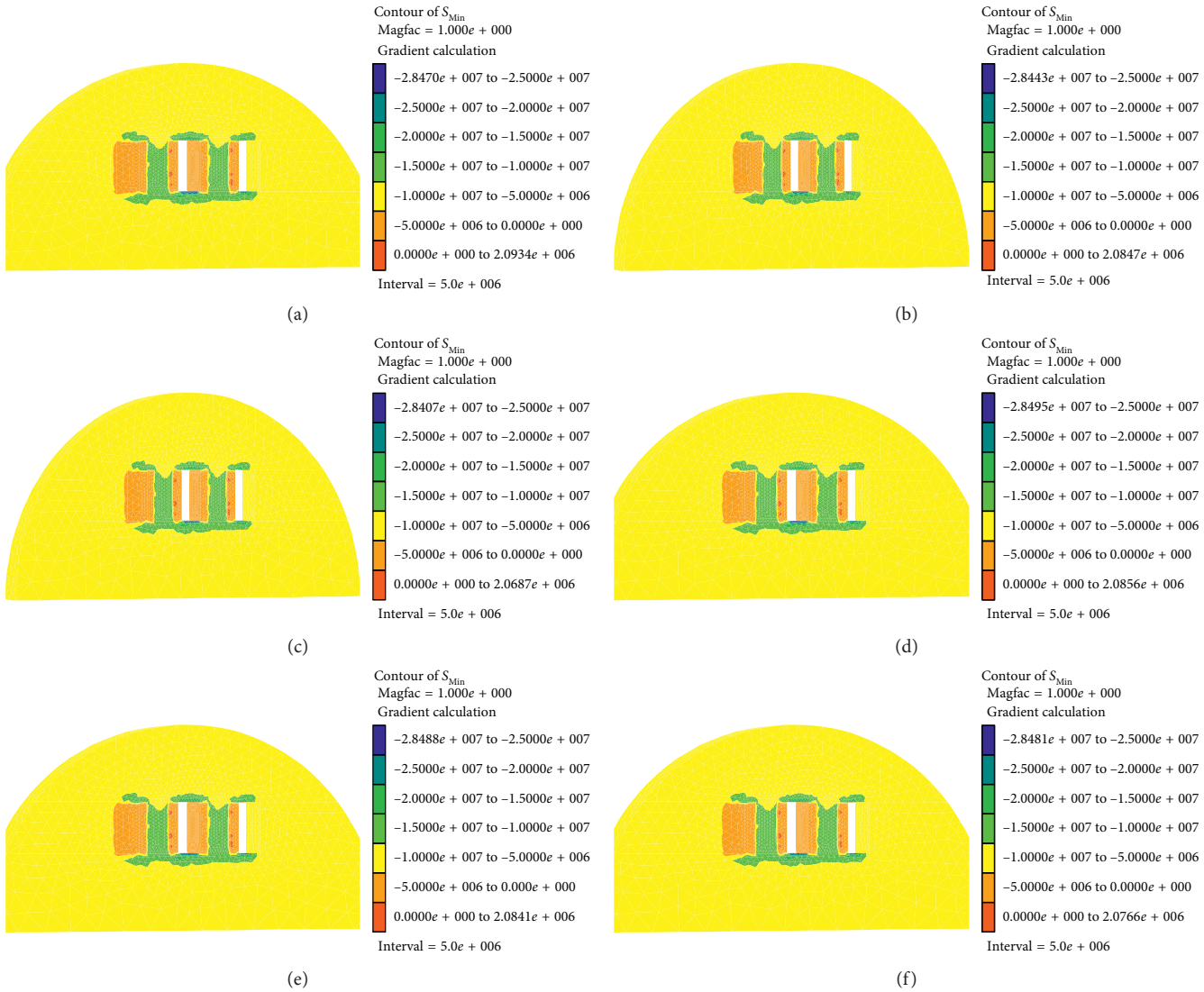

Figure 9: Minor principal stress cloud: (a) cement-sand ratio 1 : 6, backfill concentration 68%; (b) cement-sand ratio 1 : 6, backfill concentration 72%; (c) cement-sand ratio 1 : 6, backfill concentration 78%; (d) cement-sand ratio 1 : 8, backfill concentration 68%; (e) cement-sand ratio 1 : 8, backfill concentration 72%; (f) cement-sand ratio 1 : 8, backfill concentration 78%.

As shown in the minimum principal stress distribution cloud map (Figure 9), the pillar and mine mainly exhibit compressive stress. The maximum and minimum stresses of the six programs are observed at the center of the mining area and are approximately 28.4 MPa. The minimum principal stress of the surrounding rock mass is mainly concentrated at the junction of the mine house and is approximately 20 MPa. No remarkable differences are observed in the size and distribution of minimum principal stress and the compressive strength requirements for filling bodies of different proportions. This condition shows that the proportion of the filling body in this engineering environment has a small effect on the minimum principal stress of the model.

4.2.4. Comprehensive Analysis Results. The selection of the pillar filling scheme mainly considers the construction operating conditions, economic benefits, and safety factors. From the foregoing analysis, no remarkable differences are observed in the simulated effects of the six schemes in the distribution map of the plastic zone, vertical displacement, and maximum and minimum principal stresses. Filling materials account for a large part of mining costs. Therefore, the mining cost should be reduced, and the mining efficiency should be improved. And using waste tailings for filling can protect the environment. These conditions are the development trend of the filling mining method. The amount of cost savings depends on the price of cement. A small cement-sand ratio and concentration correspond to a lower amount of required cement and a lower cost. Therefore, under the premise of ensuring the stability of the mine, a smaller sand ratio and concentration correspond to the increased economy of the filling scheme. Considering the size of the damage zone shown in the plastic map and the economic savings of the project, the cemented backfill with a cement-sand ratio of 1 : 8 and concentration of 68% is the best choice.

5. Conclusion

(1) The plastic zone range of the simulated results with different filling ratios is affected by Poisson's ratio. The plastic area of the backfill is small after filling when Poisson's ratio is small. Although the six programs have exhibited a certain range of tensile damage with no obvious penetration, the safety of the stope structure can be guaranteed.

(2) No remarkable difference is observed in the displacement of the top plate subsidence and bottom plate uplift of the six schemes, and only the displacement area is slightly different.

(3) The magnitude of the maximum principal stress of the six schemes changed slightly, and the pressure and tension range of the stope structure decreased with the increase in the backfill concentration under the same cement-sand ratio. When the sand-sand ratio of the filler of the same concentration is 1 : 8, the pressure and tension range are smaller than when the cement-sand ratio is 1 : 6.

(4) The pillars and mine houses mainly show compressive stress based on the minimum principal stress cloud map. The maximum value of the minimum stress is located at the center of the mining area. A slight difference is observed between the minimum principal stress and distribution of filling bodies with different proportions, and they all meet the compressive strength requirement. This condition shows that the proportion of filling bodies has a small effect on the minimum principal stress of the model under the six schemes.

(5) On the basis of the actual situation of the mine's engineering and numerical simulation results, comprehensive consideration of economic security and other factors, the sand-sand ratio of 1 : 8 and 68% concentration of the filling body, is appropriate.

Data Availability

The test data used to support the findings of this study are included within the article.

Conflicts of Interest

The authors declare that they have no conflicts of interest.

Acknowledgments

The study has been supported by the National Natural Science Foundation (no. 51764013), by the Science and Technology Support Plan Project of Jiangxi Provincial Science and Technology Department (Grant nos. 20161BBG70075 and 20143ACG70010), and by the Key Research Project of Science and Technology of Jiangxi Provincial Education Department (Grant no. GJJ160592).

References

[1] X. X. Miao, J. X. Zhang, and G. Guo, "Study on waste-filling method and technology in fully mechanized coal mining," *Journal of China Coal Society*, vol. 35, no. 1, pp. 1–6, 2010.

[2] R. Rankine, M. Pacheco, and N. Sivakugan, "Underground mining with backfills," *Soils and Rocks*, vol. 30, no. 2, pp. 93–101, 2007.

[3] W. J. Yu and W. J. Wang, "Strata movement induced by coal-pillar under three circumstances exchange by gangue backfill and quadratic stability law," *Chinese Journal of Rock Mechanics and Engineering*, vol. 30, no. 1, pp. 105–112, 2011.

[4] Z. Zhaokai, Z. Yiping, and W. Yongming, "Research on the strength and stability on fill body of high-bench stope," *Metal Mine*, vol. 1, pp. 31–34, 2010.

[5] M. Fall and M. Benzaazoua, "Modeling the effect of sulphate on strength development of paste backfill and binder mixture optimization," *Cement and Concrete Research*, vol. 35, no. 2, pp. 301–314, 2005.

[6] M. Fall, M. Benzaazoua, and E. G. Saa, "Mix proportioning of underground cemented tailings backfill," *Tunnelling and Underground Space Technology*, vol. 23, no. 1, pp. 80–90, 2008.

[7] L. Yi-fan, Z. Jian-ming, D. Fei et al., "Experimental study on strength characteristics of tailings cement backfilling at deep-seated mined-out area," *Rock and Soil Mechanics*, vol. 26, no. 6, pp. 865–868, 2005.

[8] Z.-X. Liu, X.-B. Li, T.-G. Dai et al., "On damage model of cemented tailings backfill and its match with rock mass," *Rock and Soil Mechanics*, vol. 27, no. 9, pp. 1442–1446, 2006.

[9] Y. M. Li, C. Y. Liu, X. Z. Zou et al., "Determination and application of reasonable parameters of cemented backfilling mining technology in thin steeply inclined seam," *Journal of China Coal Society*, vol. 36, no. S1, pp. 7–12, 2011.

[10] J. M. Xu, J. X. Zhang, Y. L. Huang et al., "Experimental research on the compress deformation characteristic of waste-fly ash and its application in backfilling fully mechanized coal mining technology," *Journal of Mining and Safety Engineering*, vol. 28, no. 1, pp. 158–162, 2011.

[11] J. W. Shi, Z. J. Wei, Q. L. Liu et al., "Research on proportion optimizing of paste filling material based on orthogonal experiment in coal mine," *China Safety Science Journal*, vol. 21, no. 6, pp. 111–115, 2011.

[12] Z. Kang, Z. Hongyu, Z. Junping, W. Xiaojun, and Z. Kui, "Supporting mechanism and effect of artificial pillars in a deep metal mine," *Soils and Rocks*, vol. 39, no. 2, pp. 149–156, 2016.

[13] Z. Kang, G. Shuijie, Z. Keping et al., "Relationship between characteristics of geostress for deep mining district and mining-induced seismicity," *Electronic Journal of Geotechnical Engineering*, vol. 21, no. 22, pp. 7033–7044, 2016.

[14] J. Guo, J. Chen, F. Chen, S. Huang, and H. Wang, "Using the Schwarz alternating method to identify critical water-resistant thickness between tunnel and concealed cavity," *Advances in Civil Engineering*, vol. 2018, Article ID 8401482, 14 pages, 2018.

[15] Y. Zheng, C. Qiu, H. Zhang et al., "Exploration of stability analysis methods for surrounding rocks of soil tunnel," *Chinese Journal of Rock Mechanics and Engineering*, vol. 27, no. 10, pp. 1969–1980, 2008.